Heliyon 10 (2024) e37231

Contents lists available at ScienceDirect

Heliyon

journal homepage: www.cell.com/heliyon

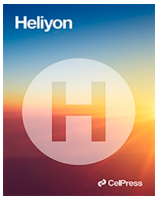

Research article

PMMA-induced biofilm promotes Schwann cells migration and proliferation mediated by EGF/Tnc/FN1 to improve sciatic nerve defect

Jun Wang [a,b], YuXuan Hu [b], Yuan Xue [b], Kai Wang [a], Dong Mao [c], Xiao-Yun Pan [c], YongJun Rui [b,*]

[a] Suzhou Medical College of Soochow University, Suzhou, Jiangsu, 215000, China
[b] Department of Orthopedics, Wuxi Ninth People's Hospital Affiliated to Soochow University, Wuxi, Jiangsu, 214000, China
[c] Orthopaedic Institute, Wuxi Ninth People's Hospital Affiliated to Soochow University, Wuxi, Jiangsu, 214000, China

ARTICLE INFO

Keywords:
Peripheral nerve
Nerve regeneration
PMMA
Silicone
Biological membrane
Tnc

ABSTRACT

Objective: The purpose of this study is to investigate the role of PMMA-induced biofilm in nerve regeneration compared with silicone-induced biofilm involved in the mechanism.
Methods: PMMA or silicon rods were placed next to the sciatic nerve to induce a biological membrane which was assayed by PCR, Western blot, immunohistochemistry, immunofluorescence and proteomics. A 10 mm sciatic nerve gaps were repaired with the autologous nerve wrapped in an induced biological membrane. The repair effects were observed through general observation, functional evaluation of nerve regeneration, ultrasound examination, neural electrophysiology, the wet weight ratio of bilateral pretibial muscle and histological evaluation. Cell proliferation and migration of Schwann cells co-cultured with EGF-treated fibroblasts combined with siRNA were investigated.
Results: The results indicated that expression of GDNF, NGF and VEGF along with neovascularization was similar in the silicone and PMMA group and as the highest at 6 weeks after operation. Nerve injury repair mediated by toluidine blue and S100β/NF200 expression, the sensory and motor function evaluation, ultrasound, target organ muscle wet-weight ratio, percentage of collagen fiber, electromyography and histochemical staining were not different between the two groups and better than blank group. EGF-treated fibroblasts promoted proliferation and migration may be Tnc expression dependently.
Conclusion: Our study suggested that PMMA similar to silicon induced biofilm may promote autogenous nerve transplantation to repair nerve defects through EGF/Tnc/FN1 to increase Schwann cells proliferation and migration.

1. Introduction

The vast majority of peripheral nerve defects are caused by severe trauma or tumor infiltration [1]. These conditions usually result in decreased motor function and sensory perception, which affect a patient's quality of life and ability to work. Peripheral nerve

* Corresponding author. Department of Orthopedics, Wuxi Ninth People's Hospital Affiliated to Soochow University, Wuxi, Jiangsu, 214000, China.
E-mail address: wxjyegk123456@126.com (Y. Rui).

https://doi.org/10.1016/j.heliyon.2024.e37231
Received 10 April 2024; Received in revised form 14 August 2024; Accepted 29 August 2024
Available online 2 September 2024

Abbreviations

PMMA	polymethyl methacrylate
VEGF	vascular endothelial growth factor
NGF	nerve growth factor
GDNF	glial cell line-derived neurotrophic factor
IGF	insulin-like growth factor
FN1	Fibronectin
EGF	epidermal growth factor

regeneration for long nerve defects is the most challenging aspect of the treatment of peripheral nerve injury, and numerous studies employing various approaches have been undertaken [2]. Although various treatments have recently been developed to replace autologous nerve grafts. Currently, no other graft material can compete with autologous nerve, a technique that preserves the anatomical integrity of the injured nerve and has been recognized as the "gold standard" [3]. For long segmental nerve defects, conventional nerve grafts are prone to ischemic necrosis [4]. In order to form an internal environment around the anastomosis that is conducive to peripheral nerve regeneration, biological membrane is usually used to wrap around the anastomosis to form a physical barrier to prevent adhesion and scar formation between the anastomosis and surrounding tissues after surgery. The traditional Masquelet induced membrane technique has been followed by using polymethyl methacrylate (PMMA) bone cement as the induced membrane medium. Because the inflammatory response induced by bone cement is milder than other materials, the use of silicone will produce strong T cell and macrophage responses [5]. In addition, PMMA is a local antibiotic carrier for treatment of infections [6], and appropriate concentration of antibiotics can improve the activity of PMMA induced membrane. Masquelet's induced membrane technique (MIMT) is a relatively new, two-stage surgical procedure to reconstruct segmental bone defects. The reconstruction technique involves two surgical steps: in the first step, PMMA is inserted into the bone defect and the proximal and distal segments are held together. Over the next six weeks or so, PMMA is coated with induced membranes (IM). In the second step, the cement spacer was removed (after a careful cement incision) and non-vascularized autogenous cancellous bone was filled [7].

The idea of using a silicon pseudo synovial sheath for nerve repair was first proposed by Lundborg [8]. Subsequently, silicone induced membrane has been used as an empty conduit to treat nerve defects with good results [9–11]. Synthetic non-degradable polymer silicone is one of the first used materials for nerve repair. However, silicone materials have many disadvantages, such as non-degradability, large inflammatory reaction and scar formation, which are not conducive to the regeneration of peripheral nerve injury, so they are gradually eliminated from use. Takeuchi et al. used a silicone induced biofilm to wrap nerve grafts to treat nerve defects and obtained good axonal regeneration. The authors note that PMMA or titanium can also be used instead of silicone [12]. In addition, PMMA provides mechanical stability and can be easily supplemented with various antibiotics in various dosages to treat deep infections [13].

Ozalp was the first scholar to propose a method based on Masquelet technique for the treatment of bone defects for the repair of nerve defects [14]. Subsequently, some scholars also proposed that Masquelet technique could be simulated for two-stage nerve transplantation to treat nerve defects [15]. PMMA can also induce a biofilm in muscle that is also rich in neovascularization [16]. There have been related reports on the study of PMMA and silicone induced membrane on bone regeneration in bone defects and subcutaneous [17,18]. However, the relevance of PMMA-induced biofilms in the treatment of nerve defects has not been reported. The purpose of this study is to investigate whether PMMA-induced muscle biofilm contains nerve growth related factors and whether its histological characteristics are different from those of silicon-induced muscle biofilm. Moreover, the role of PMMA-induced biofilms in a rat sciatic nerve defect model was also evaluated and the mechanisms by which biofilms promote nerve regeneration was explored.

2. Materials and methods

2.1. Materials and antibodies

Silicone rods were prepared by our laboratory. PMMA were purchased from Stryker (Kalamazoo, Michigan, USA). siRNA and negative control (NC) were designed online (https://www.invivogen.com) and synthesized by Sangon Biotech (Shanghai, China). Antibodies of NGF (ab6199, Abcam) VEGFA (ab214424, Abcam), GDNF (ab28956, Abcam), Vimentin (ab92547, Abcam), S100β (ab52642, Abcam), NF200 (ab215903, Abcam) and CD31 (ab204527, Abcam) were purchased from Abcam (Cambridge, MA UK). Antibodies of IGF (28530-1-AP, Proteintech), Tnc (67710-1-Ig, Proteintech), FN1(15613-1-AP, Proteintech) and β-actin (66009-1-Ig, Proteintech) were supplied by Proteintech Group (Wuhan, China), Inc. Primary antibody of EGF (sc-374255, Santa) was purchased from Santa Cruz Biotechnology (Santa Cruz, CA, USA)., Inc.

2.2. Experimental design

Following Local Ethical Board approval, seventy-five adult female rats (SD rats, 10–12 weeks, 250–300 g) were used for this study. SD rats were intraperitoneally injected with sodium pentobarbital of 5 g/500 mL or 0.4 mL at the rate of 40 mg/kg. CD31 staining of biological membrane was performed in 18 rats at 4, 6, and 8 weeks. Thirty-six rats were used to measure the amount of nerve growth

related factors in the induced membranes for different weeks. The 18 rats were used to evaluate the efficacy of the two materials induced membrane wrapped autologous nerve grafts in repairing nerve defects. Induced membranes were obtained in the first stage of surgery as described below. In the second stage, the nerve regeneration was observed and evaluated at 8 and 12 weeks after operation.

2.3. Biofilm induction in vivo and factors and vascularization detection

In the first part, 18 rats were used for CD31 staining, and the other 36 rats were used for PCR and WB detection. Sixty rats were divided into two groups, 30 rats in each group. In the PMMA group, a 15 mm PMMA spacer (13 mm in length and 2.5 mm in diameter) was placed parallel to the sciatic nerve (Fig. 1, left). The ends of the PMMA were fixed within the muscle tissue to prevent sliding from affecting the formation of the induced membrane. In the silicone group, a 13 mm long and 2.5 mm diameter silicone spacer was placed parallel to the sciatic nerve (Fig. 1, right), and was fixed to the muscle tissue in the same manner. After 4, 6, and 8 weeks, we observed the biofilm induced by different materials at different weeks under the microscope. Three rats from each group were used for PCR, three rats for WB, six rats for proteomic analysis and another three rats for CD31 staining.

2.4. In vivo prefabrication of two kinds of membrane materials and autologous nerve transplantation

An oblique incision approximately 3 cm long was made along the posterior lateral side of the right thigh to expose the right sciatic nerve. The sciatic nerve defect model was prepared by cutting and excising the sciatic nerve approximately 1 cm long at the lower margin of the piriformis muscle 5 cm away. The nerve defect was repaired with different methods. For the PMMA group, two small openings were cut at both ends of the membrane, the PMMA was taken out without harming the membrane, and the autologous nerve was rotated 180° before being inserted into the membrane (Fig. 2A). For the silicone group, silicone was taken out and otherwise the same as that in the PMMA group (Fig. 2B). For the blank group (Fig. 2C), the first stage is suturing the wound after incision of the skin to expose the middle sciatic nerve. The second stage is the same method as above, the autogenous nerve was rotated 180°. The excised sciatic nerve segment was repaired between the proximal and distal stump using 10–0 nylon epineural interrupted sutures.

2.5. Detection method and evaluation index

2.5.1. General observation

The systemic and local wound conditions of the three groups were observed at different time points after surgery, and the position, area, depth and final healing of postoperative foot ulcers were compared among the three groups. At 8 and 12 weeks after operation, the anastomosis and angiogenesis of the grafted nerve were observed, and the adhesion degree of the grafted nerve to the surrounding

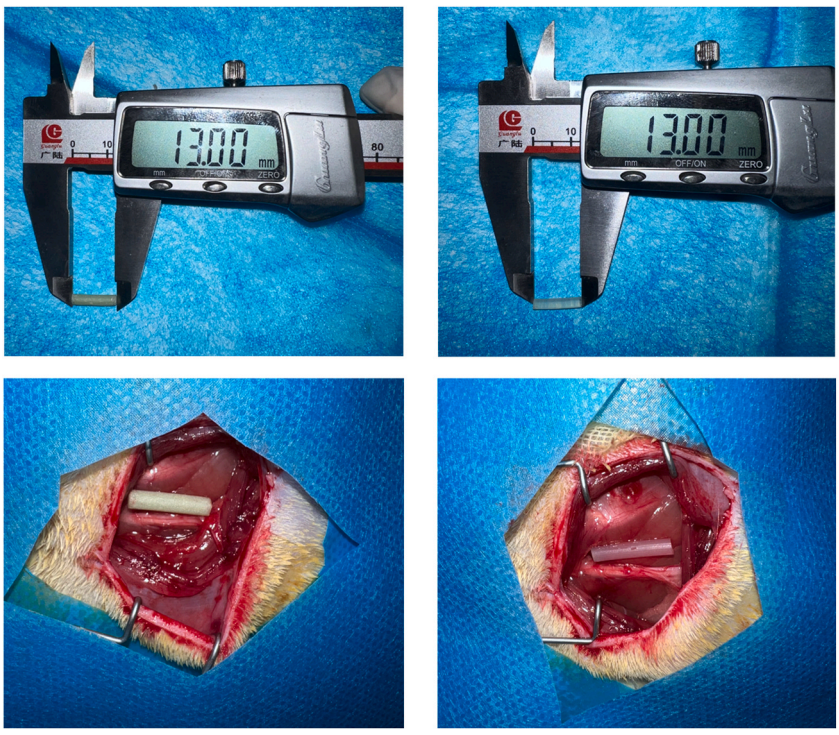

Fig. 1. Placement of PMMA (left) and silicone spacer (right). The PMMA and silicone spacer with 13 mm in length and 2.5 mm in diameter was placed parallel to the sciatic nerve.

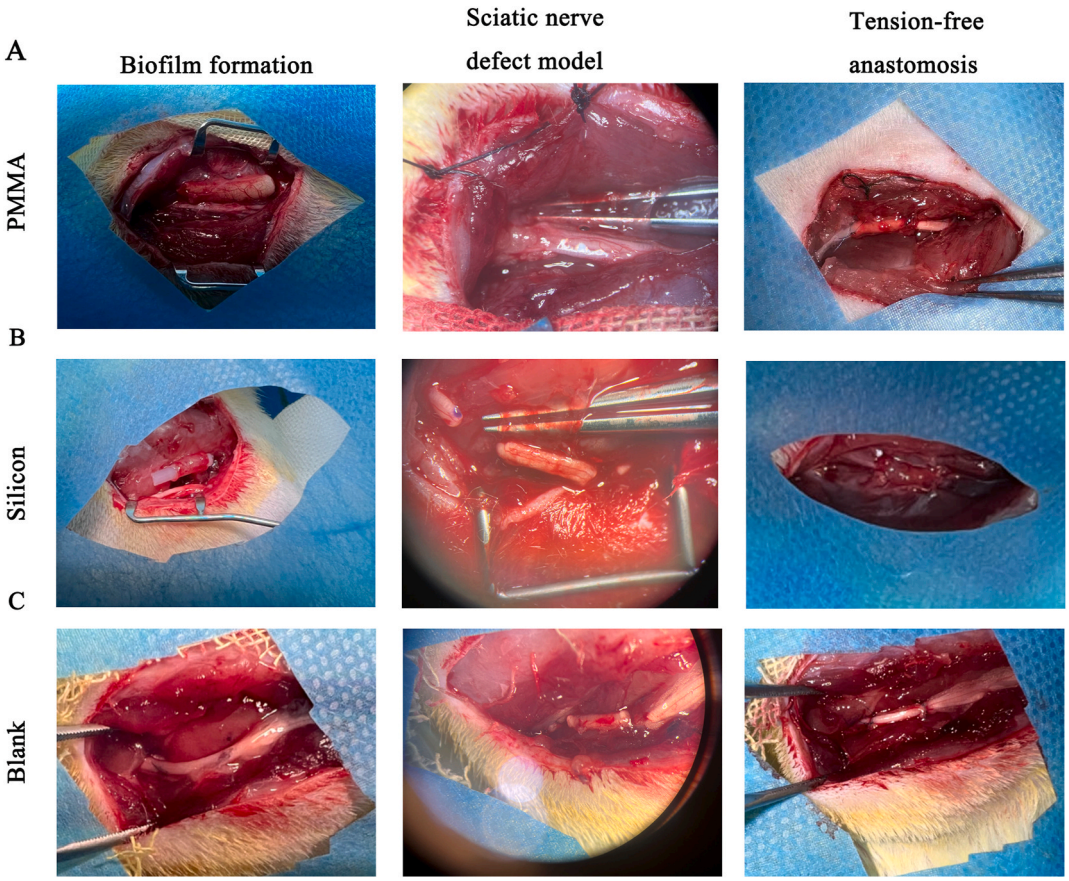

Fig. 2. Representative images of in vivo prefabrication of two kinds of membrane materials and autologous nerve transplantation. The three images on the far left panel, from top to bottom, are biofilm formation 6 weeks after PMMA placement (A), 6 weeks after silicone placement (B), and blank group (C). In the middle panel, a 1-cm sciatic nerve defect model was made 5 mm below the inferior border of the piriformis muscle, and the nerve was turned over, and the PMMA group and the silicone group were stuffed into the biofilm. The rightmost group had a tension-free anastomosis at both ends.

tissue was evaluated according to the classification proposed by Lodge et al. [19]. The degree is as follows: Grade 0: no adhesion; Grade 1: Loose filmy adhesions separable through blunt dissection; Grad 2: Less than 50 % of adhesions requiring separation through sharp dissection; Grade 3: More than 50 % of adhesions requiring separation through sharp dissection; Grade 4: Severe adhesion; Grade 5: Full-thickness adhesion.

2.5.2. Sensory and motor function detection of nerve regeneration

At 8 and 12 weeks after surgery, sensory and motor functions of rats were measured by pinprick test and the toe-spread test, the results were scored as grade 0 to 3 [20]. The recovery of sensory function was detected by pinprick test. The contractile response of the rat foot was observed by pinprick the foot. It is scored from 0 to 3, with higher levels indicating better pain and tactile recovery. The recovery of motor function was assessed by means of toe extension tests. The rats were graded by observing abduction and hyper-extension when suspended by the tail. The higher the series, the better the recovery.

2.5.3. Neural electrophysiology

At 8 and 12 weeks after surgery, the rats were anesthetized, and the nerve graft segments were exposed by skin incision and dissected proximally and distally. The sciatic nerve proximal to the proximal anastomosis was electrically stimulated with a pair of bipolar hook electrodes, and a unipolar needle recording electrode was inserted into the ipsilateral gastrocnemius muscle belly while a ground electrode was inserted into the dorsal skin. A hypermaximal stimulus (1 mA in intensity) was administered to evoke the maximal CMAP response. The records were repeated three times and averaged. Motor nerve conduction velocity (NCV) was calculated by dividing the distance difference between the proximal and distal ends of the stimulated site by the latency difference. To avoid muscle jitters caused by cold stimulation, the laboratory temperature should be controlled.

2.5.4. Wet weight ratio of pretibial muscle

The rats were sacrificed at the end of electrophysiological examination at 8 and 12 weeks after nerve transfer, and bilateral tibialis

anterior muscles were harvested. Then, the wet weight was determined using an electronic balance. The wet weight ratio of the anterior tibial muscle on the affected side was calculated by comparing the weight of the anterior tibial muscle on the experimental side and the normal side.

2.5.5. qPCR assay

Total RNA was isolated from the samples firstly, and then reverse transcription, amplification and detection on a fluorescent quantitative PCR instrument were performed in turn. The primers of VEGFA, NGF, GDNF and IGF were showed in Table 1. $2^{-\Delta\Delta CT}$ method was used to quantify the relative mRNA expression to β-actin.

2.5.6. Protein expression assayed by western blot analysis (WB) and ELISA

The protein expression of VEGFA, NGF, GDNF, IGF, Tnc and FN1 in the biological membrane tissue was measured using western blotting. In brief, total protein of the samples was extracted and then SDS-PAGE electrophoresis was performed to isolate the proteins which were transferred to PVDF membrane followed by incubation with primary antibodies of VEGFA (1:500), NGF (1:200), GDNF (1:500), IGF (1:200), Tnc (1:500), FN1(1:500) or β-actin (1:5000) in the darkroom at 4 °C overnight. The membrane was incubated with corresponding second antibodies for 2 h at room temperature. Then the membrane was added ECL chemiluminescence solution and the images were taken under a chemiluminescence imager. The internal reference protein was β-actin. The gray value of each strip was analyzed by ImageJ software, and the statistical analysis was carried out. The levels of EGF in the membrane were quantified by ELISA according to the introduction of the kits.

2.5.7. Immunohistochemistry

CD31 expression was used to evaluate vascularization degree in the biological membrane. Paraffin sections were processed by continuous rinsing (100 % xylene, three times for 20 min; 100 % alcohol, 5 min; 95 % alcohol, 5 min; 85 % alcohol, 5 min; 75 % alcohol, 5 min; Distilled water, 5 min), followed by antigen repair by incubation with primary antibody of CD31 and then with suitable secondary antibody. The sections were observed under a microscope and photographs were taken (400× magnification).

2.5.8. Immunofluorescence detection

S100β and Neurofilament 200 (NF-200) staining of cross-sections of the samples was used to observe the regeneration of axons and Schwann cells. The samples were paraffin sectioned firstly and then the sections were undergone antigen retrieval, incubation with primary antibodies of S100β (1:100) and NF-200 (1:50) followed by incubation with fluorescent probe labeled secondary antibodies. The sections were observed under a fluorescence microscope.

EGF co-expression with Vimentin, a marker of fibroblasts in the biological membrane was detected using immunofluorescence. Similarly, the samples were paraffin sectioned firstly and then the sections were undergone antigen retrieval, incubation with primary antibodies of EGF (1:50) and Vimentin (1:100) followed by incubation with fluorescent probe labeled secondary antibodies. Photographs were taken under a fluorescence microscope.

2.5.9. Masson's trichrome staining

Masson's trichrome staining was performed to investigate the muscle recovery after nerve transplantation. The samples were fixed overnight with 4 % paraformaldehyde, then dehydrated, embedded and followed by Masson reagent staining to observe the fibers and collagen. Photographs of the sections with a 200× magnification were taken under a microscopy.

2.5.10. Toluidine blue staining

The nerve samples were fixed in 4 % paraformaldehyde, embedded in paraffin wax. The semi-thin sections were obtained using a microtome followed be staining with toluidine blue and observed under an optical microscope. The total area and number of myelinated nerve fibers were measured by Image-Pro Plus software. Three images were randomly collected from each specimen to count the number of medullated nerve fibers.

Table 1
Primers for PCR assay.

Gene	Primers Sequence (5'->3')	Product (bp)
VEGFA	Forward: TTCGTCCAACTTCTGGGCTC Reverse: GCTTTCTGCTCCCCTTCTGT	**172**
NGF	Forward: GAGCGCATCGCTCTCCTT Reverse: GTGTGAGTCGTGGTGCAGTA	**776**
GDNF	Forward: ACACTCGAGGAGGAAGGACA Reverse: CGGCAGTCCCTTGAAGACAT	**438**
IGF	Forward: GACGTACCAAAATGAGCGCACC Reverse: TCGATAGGGGCTGGGACTTC	**381**
Actb	Forward: GTCCACCCGCGAGTACAAC Reverse: GGATGCCTCTCTTGCTCTGG	**260**

2.5.11. Proteomic assay

Label-free whole proteomics assay of the biological membrane (4weeks, 6weeks and 8weeks) and bioinformatics analysis was performed (Majorbio). Briefly, based on the RAW files detected by mass spectrometry, the corresponding species protein database was searched and compared. Based on the database search results, mass tolerance distribution analysis of peptide, protein and parent ion was performed to evaluate the quality of the mass spectrometry detection data. Protein identification and quantitative analysis were performed on the screened proteins after quality control, and a rough-sample protein statistics was obtained. Then we screen the

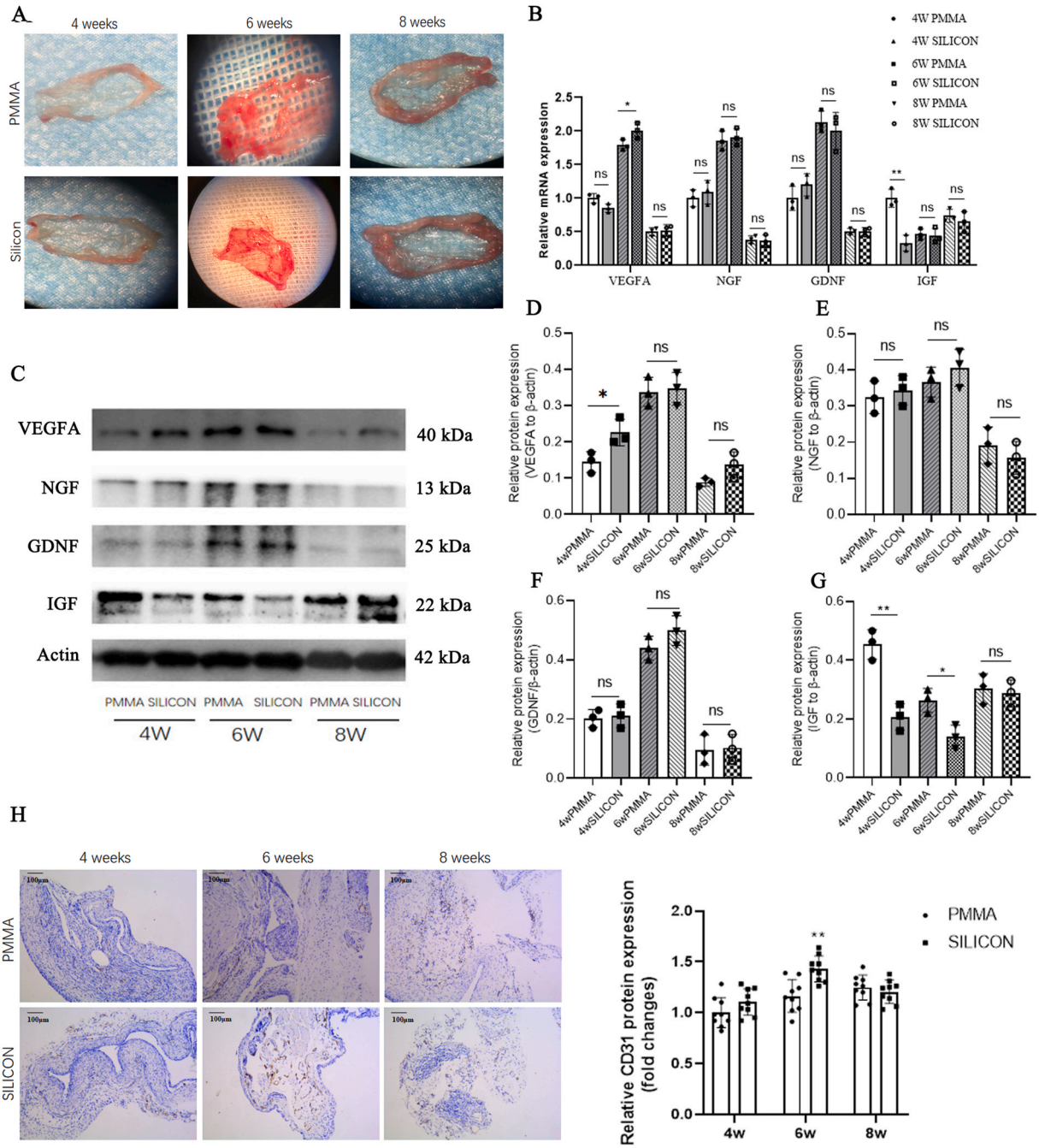

Fig. 3. Biofilm characteristics (A) Images of the induced-membranes at 4, 6, and 8 weeks. (B) PCR were performed to analysis the content of neuro-related factor-VEGFA, NGF, GDNF and IGF. (C) Images of the blots of VEGFA, NGF, GDNF and IGF in the induced-membranes at 4, 6, and 8 weeks. (D) Statistical analysis of VEGFA expression assayed by western blots. (E) Statistical analysis of NGF expression assayed by western blots. (F) Statistical analysis of GDNF expression assayed by western blots. (G) Statistical analysis of IGF expression assayed by western blots. (H) CD31 staining was used to show the number of new blood vessels. n = 3. ns, no significance; $^{*}P < 0.05$, $^{**}P < 0.01$.

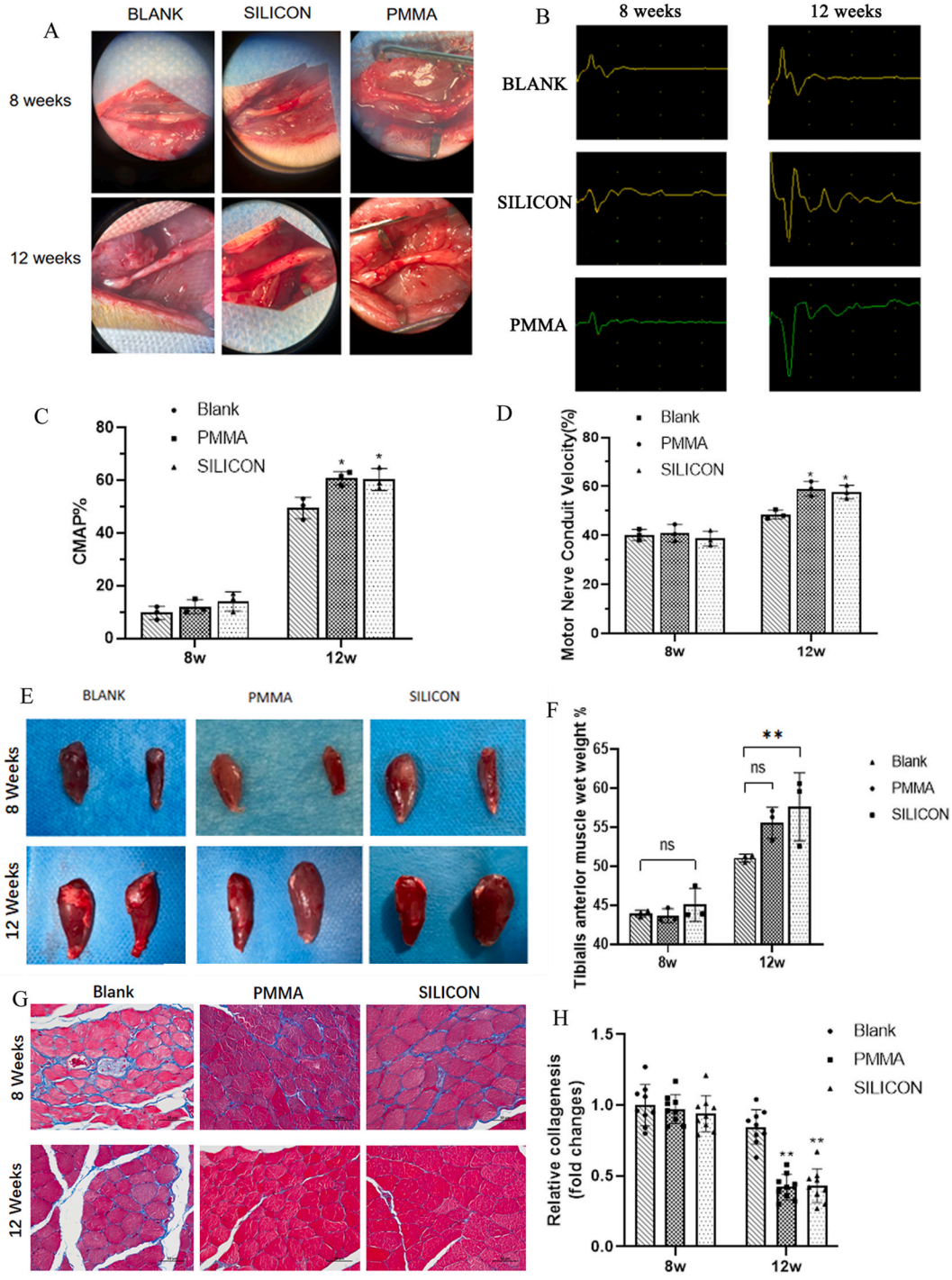

Fig. 4. Morphological observation, Electrophysiological evaluation and Evaluation of target muscle reinnervation. (A) Morphological observation and degree of vascularization on the surface of the transplanted nerve at 8 and 12 weeks after operation. (B) Electrophysiological evaluation of different groups at 8 and 12 weeks after nerve grafting. (C) Representative CMAP recordings at the injured side in each group at 8 and12 weeks after the nerve autograft. CMAP. (D) NCV were calculated. n = 3. ns, no significance; $^{*}P < 0.05$ compared with blank. (E) Evaluation of target muscle reinnervation and representative images. (F) The wet weight rate of tibial anterior muscle in each group at 8 and12 weeks after the nerve. (G) Masson staining of the tibialis anterior muscle on the affected sides was used to measure the muscle atrophy of the target organ of sciatic nerve injury. (H) Quantitative analysis of collagen fibers by Masson staining. n = 3. $^{**}P < 0.01$ compared with blank.

differential proteins and analyze the proteins with the required multiple of difference.

2.6. Experiments in vitro

2.6.1. Cells, cell culture and treatment

Rat Schwann cells RSC96 were purchased from Cell Bank, Chinese Academy of Sciences and cultured in DMEM supplied with 10 % fetal bovine serum (FBS) in an incubator with 5 % CO_2 and 95 % atmosphere. Rat synovial fibroblasts (rFLS) were isolated from synovium of rats (male, 150 ± 20 g) which were cultured in DMEM medium. 10 ng/mL EGF was used to treat rFLS which was plated in the subcellular chamber (Transwell) co-cultured with RSC96 in the upper chamber.

2.6.2. Proliferation assay

After co-cultured with rFLS for 12, 24, 48 and 72 h, RSC96 cells were added with 10 μl CCK8 solution and incubated at 37 °C for another 2 h, optical density value at 450 nm (OD450nm) was obtained using a microplate reader.

2.6.3. Migration assay

After co-cultured with rFLS for 24 h, RSC96 cells in the upper chamber were in FBS-free culture and placed in a suitable orifice plate containing complete medium with 10 % FBS at 37 °C for another 8 h incubation. After then, the migrated cells were stained using crystal violet and cells photographs were taken under a microscope.

2.7. Statistical analysis

Statistical analysis was performed using Graph Pad Prism 8.0 software (Graph Pad software, La Jolla/CA, USA). Descriptive results are detailed as means and standard deviations. One-way ANOVA, nonparametric Kruskal-Wallis test for rank-sum ANOVA, and Dunn's test for multiple comparisons were used. The *t*-test was used to compare the physiological data of irradiated and non-irradiated rats. Image-Pro Plus (IPP) software was used to determine the positive level of each protein in the immunofluorescence or immunohistochemical specimen. Three fields were randomly selected, and the integral optical density (IOD) value of positive protein expression in the region of interest (ROI) was divided by the area of the selected region of interest, that is, the average optical density value was used as the positive protein expression level, and the mean value of the three was used as the final statistical result of each sample. The $P < 0.05$ indicates that the difference is statistically significant.

3. Results

3.1. Expression of neurotrophic factors and angiogenesis in biofilms

Microscopically, the most obvious vascularization of the biofilm was observed at 6 weeks, and there was no significant difference in the degree of vascularization between the PMMA group and the silicone group (Fig. 3A). The results of PCR (Fig. 3B) and WB (Fig. 3C–G) showed that there was no significant difference in the contents of VEGF, NGF, and GDNF between the two membrane groups at 6 and 8 weeks. The protein content of IGF was higher in PMMA induced films than that in silicone induced films at 4 and 6 weeks. Relative quantitative analysis of CD31 staining showed that the number of new blood vessels in the PMMA group was less than that in the silicone group at 6 weeks, but there was no significant difference between the two groups at 4 and 8 weeks (Fig. 3H). The number of factors, except for IGF, and vessels was the highest at 6 weeks.

3.2. Evaluation of function recovery, neural electrophysiological and target muscle reinnervation in sciatic nerve defect model

The healing time of plantar ulcers in PMMA group and silicone group was 5 weeks after surgery, and in blank group was about 6 weeks after surgery. There was no significant difference in the healing rate of foot skin ulcer among the three groups. No nerve graft was deformed. Eight weeks after surgery, there was no significant difference in the degree of nerve edema among the three groups. At 12 weeks after operation, there was no obvious edema of nerve grafts in the material group, and the nerve fiber bundles were clearer than those in the blank group. The nerve grafts in the three groups were well anastomosed with the peripheral nerve stumps, and no neuroma was observed at the anastomosis site. The nerve grafts were well anastomosed with the peripheral nerve stumps in the three groups, and no neuroma was found at the anastomosis site. The nerve grafts in PMMA group and silicone group had mild adhesion to the surrounding tissue, which was grade 0 according to the adhesion grading standard. In blank group, the adhesion between the transplanted nerve and the surrounding tissue was severe, which was grade 3. At 8 and 12 weeks after operation, the degree of vascularization of the nerve grafts in the two material groups was more obvious than that in the blank group (Fig. 4A).

Eight weeks after surgery, the Pinprick test and Toe-spread test in the three groups were poor, with 3 rats having 1 rat of grade 1 and 2 rats of grade 0 (Table 2). Twelve weeks after surgery, two of the three rats were grade 3 and one was grade 2 in the Pinprick test and Toe-spread test in the PMMA group and the silicone group. In the blank control group, 1 was grade 3 and 2 was grade 2 in the Pinprick test, and all three rats were grade 2 in the Toe-spread test (Table 3).

Electrophysiological evaluation showed that there was no statistically significant difference in CMAP% (Fig. 4B and C) and NCV% (Fig. 4D) between the three groups at 8 weeks postoperatively. At 12 weeks postoperatively, there was no statistically significant difference in CMAP% and NCV% between the PMMA group and the silicone group; but both were significantly higher than the blank

group.

Eight weeks after nerve transplantation, the wet weight rate of the tibial anterior muscle on the affected side in PMMA group (42.87 ± 1.65 %), silicone group (45.7 ± 1.47 %), and blank group (43.83 ± 0.70 %) was not significantly different. At 12 weeks after operation, the wet weight rate of target organ muscle in PMMA group (57.97 ± 1.73 %) and silicone group (57.33 ± 3.43 %) was higher than that in blank group (50.82 ± 0.93 %), and the difference was statistically significant. There was no significant difference between the two groups (Fig. 4E and F). Masson staining showed that there was no significant difference in the percentage of collagen fibers among the three groups at 8 weeks after operation (Fig. 4G and H). At 12 weeks after operation, there was no significant difference in the area percentage of collagen fibers between the PMMA group and the silicone group, but the area percentage of collagen fibers in the two material groups was significantly lower than that in the blank group.

3.3. Evaluation of nerve regeneration

Toluidine staining (Fig. 5A and B) showed that the number of regenerated myelin axons in the PMMA group and the silicone group was more than that in the blank group at 8 and 12 weeks after operation, and the difference was statistically significant. There was no significant difference between the two materials groups.

The immunofluorescence staining results of the middle (Fig. 5C) and distal (Fig. 5D) anastomosis of the transplanted nerve showed that the staining intensity of the two materials groups was significantly higher than that of the blank control group at 8 and 12 weeks after operation, and the difference was statistically significant. There was no significant difference in staining intensity between the two material groups.

3.4. Proteomic analysis reveals differential expression of Tnc and associated factors in biofilms during nerve regeneration

In order to further explore the mechanism of biofilm promoting nerve regeneration, proteomics assay was performed and results were showed in Fig. 6. There are 3931 proteins were found in the biological membrane of 4, 6 and 8 weeks induction (Fig. 6A–B). Tnc was among the differential proteins ($|\log2(FC)|>1$, $P < 0.05$) which was upregulated in the 6-week biological membrane compared with 4-week one (Fig. 6C) and was downregulated in 8-week biological membrane compared with 6-week one (Fig. 6D). The differential proteins involved in biological processes (BP) such as peripheral nervous system axon regeneration and collagen fibril organization (Fig. 6E). Tnc expression were the highest in the 6-week biological membrane and there was no significant difference between 4-week and 8-week biological membrane (Fig. 6F). Results of bioinformatics analysis showed that Tnc may be associated with EGF/EGFR and FN1 which were involved in cell proliferation, cell adhesion and migration processes (Fig. 6G).

To explore the role of EGF/Tnc/FN1 in the biological membrane and association with nerve regeneration, the levels of EGF/Tnc/FN1 in the biological membrane were detected in the present study. As showed in Fig. 7A–C, the protein levels of Tnc, FN1 and EGF were significantly upregulated in the 6-week biological membrane compared with the 4-week one which was downregulated in the 8-week membrane. Results of immunofluorescence colocalization protein detection showed that EGF co-expressed with Vimentin, a marker protein of fibroblasts was the highest in the 6-week biological membrane which was downregulated in 8-week biological membrane significantly (Fig. 7D–E). The relation of fibroblasts secreted EGF with proliferation and migration of Schwann cells were then investigated in the followed study. It was showed in Fig. 7F–G that EGF-treated rFLS induced increasing migration ability of Schwann cells and siTnc attenuated the effect of rFLS on Schwann cells migration. It was similarly to cell proliferation that EGF-treated rFLS induced increasing cell proliferation of Schwann cells which was alleviated by siTnc expression (Fig. 7H).

4. Discussion

Schwann cells, stromal membrane, neurotrophic factors, and good blood supply constitute the microenvironment of nerve regeneration. After peripheral nerve injury, a good nerve regeneration microenvironment is beneficial to protect damaged neurons and promote effective axon regeneration [20]. Polymethyl methacrylate (PMMA) is an organic polymer extensively utilized in medical polymer materials and electronic devices due to its excellent chemical stability, superior dielectric properties, and electrical insulation capabilities [21,22]. PMMA induced biofilm can provide a good environment for the growth of second-stage graft bone [23]. Some scholars believe that the induced membrane provides a better microenvironment for the regeneration of axons and Schwann cells [9,11]. In the present study, in 10 mm rat sciatic nerve defect model, PMMA and silicone induced membrane can create good environment for neural transplantation, and both materials can achieve the same axonal regeneration effect, histological and functional results to achieve the ultimate goal of peripheral nerve repair strategy, which is to maximize functional recovery and shorten recovery time [24]. Silicone membranes produce in the animal model membranes with similar characteristics to that of PMMA. However, this material has

Table 2
Evaluation of function recovery 8 weeks after surgery.

NO.	BLANK			SILICON			PMMA		
	#1	#2	#3	#1	#2	#3	#1	#2	#3
Pinprick	1	0	0	0	0	1	0	0	0
Toe-spread	1	0	0	0	1	0	0	0	1

Table 3
Evaluation of function recovery 12 weeks after surgery.

NO.	BLANK			SILICON			PMMA		
	#1	#2	#3	#1	#2	#3	#1	#2	#3
Pinprick	3	2	2	3	3	2	3	2	3
Toe-spread	2	2	2	3	2	3	2	3	3

never been used in clinical practice for a Masquelet procedure and bone healing has not been evaluated until now [25].

Several studies have reported that the essential components for nerve regeneration [26,27] include vascularity supportive cells [28], and growth factors [29,30]. The deficiency of vascularization and growth factor is the key factor restricting the success of its repair. Silicone rod-induced biofilms provide a soft lumen, good vascularization, and a stable structure that can be effectively used to encapsulate nerve graft segments [15]. There have been several trials to enhance nerve regeneration by using growth factors such as NGF, IGF and VEGF in direct repair or acellular nerve allograft models [30–32]. In this study, the results of WB showed that NGF, VEGF, IGF and other nerve regeneration related factors were contained in the induced membranes of the two groups, which confirmed the conjecture of Abdul et al. [11,33]. The IGF content in PMMA group was significantly higher than that in silica silicon group. Combined with the results of subsequent experiments, it is suggested that IGF has little or no effect on nerve regeneration, and the inducement of membrane to promote nerve regeneration may be related to the content of VEGF, NGF and GDNF. The proteomic results showed that Tnc may be one of differential proteins in the biological membrane induced for 4, 6 or 8 weeks and the highest Tnc expression was found in 6-week membrane. The following bioinformatics analysis showed that EGF and FN1 involved in cell proliferation [34] and migration [35] may be associated with Tnc which was then explored in the present study. EGF and its receptor EGFR may be expressed in fibroblasts contributing to recovery of the severed peripheral nerve in rats [36]. The relation of fibroblasts with cell proliferation and migration of Schwann cells was investigated, and results demonstrated that EGF-treated fibroblasts promoted proliferation and migration may be Tnc expression dependently which may be consistent with the previous study [37]. Moreover, we can see more mature blood vessels with CD31 [38] and there are abundant neovascularization in the membrane, especially in the 6-week induced membrane, the neovascularization content in the induced membrane was similar between the two groups, which provides a rich nutrition for the transplanted nerve.

Scarring near the nerve graft may cause the compression of nerve fibers with the scar tissue, which has a deleterious effect on the functional outcome after nerve repair and may result in persistent paresthesia, pain, or incomplete motor return [39]. In this study, the blank group appeared to have the most severe adhesion near the repaired nerves, whereas PMMA group and silicon group had significantly less adhesion than the blank control group did. This is consistent with Abdulaziz's report [40] that silicon rod-induced biofilm formation minimizes fibrosis-induced adhesion.

The goal of treatment for large peripheral nerve defects is to restore critical function and sensitivity of the limb [41]. In the present study, we used the pinprick test and the toe-spread test [42] to evaluate the functional recovery of sensory and motor nerves in the three groups at 8 and 12 weeks. At 8 weeks after operation, the material group did not play a significant role. Twelve weeks after operation, the material groups, the PMMA group and the silicone group, effectively promoted the functional recovery of the affected limb and improved its sensitivity compared with the simple autogenous nerve transplantation.

Amplitude and NCV are two important indexes for detecting the recovery of the function in injured peripheral nerve [43]. NCV can reflect the degree of impairment in the nerve myelin sheath [44]. It is also an important indicator of nerve fiber maturity [45]. This study demonstrated that biofilm significantly promoted the maturation of transplanted nerve fibers at 12 weeks.

Due to the slow recovery of peripheral nerve injury, different degrees of muscular atrophy will occur in the affected innervated area regardless of the transplantation method [46]. After peripheral nerve repair, the re-innervation of nerve fibers to target muscles is an important factor affecting nerve function [47]. The methods to evaluate the recovery of sciatic nerve function were target muscle wet weight rate and Masson staining. At 12 weeks postoperatively, the area and wet weight ratio of collagen fibers in the two groups were similar, and were significantly higher than those in group C, indicating that the biofilm induced by the nerve grafts wrapped by the two groups could effectively inhibit the formation of fibrotic tissue to the same extent, and alleviate partial loss of skeletal muscle atrophy after denervation at 12 weeks.

Toluidine blue staining showed that induced of membrane-wrapped transplanted nerves from 8 weeks after surgery could promote cell proliferation and axon regeneration. The S100β and NF-200 (marked for neurofilaments for axonal tracing) were performed in an immunofluorescence assay to further evaluate the axon growth [48]. The intensity of S100β protein and NF-200 in PMMA group and silicon group was higher than that in blank group, indicating that there were more newly formed neural tissues in material group than in blank group at 8 and 12 weeks after the operation.

The interval between the two stages of surgery varies among different scholars. Ozalp et al. simulated the Masquelet technique by putting silica silicon into the nerve side to form a biofilm in the second stage. Five weeks later, the membrane was used to wrap the nerve to repair the nerve defect, and good functional recovery was obtained [14]. Subsequently, a second operation at 4 weeks was studied, which also demonstrated that the biofilm produced by silicon could enhance the vascularity of the graft and improves functional recovery [15]. Takeuchi had a second surgery after eight weeks of silicone placement, also demonstrating that vascularized biogenic conduits of the biological catheter with blood could promote the regeneration of the transplanted nerve and can offer superior functional and morphological recovery of regenerated axons [12]. This study demonstrated that the biofilm was most active at 6 weeks. We recommend an interval of 6 weeks between the two nerve transfer procedures.

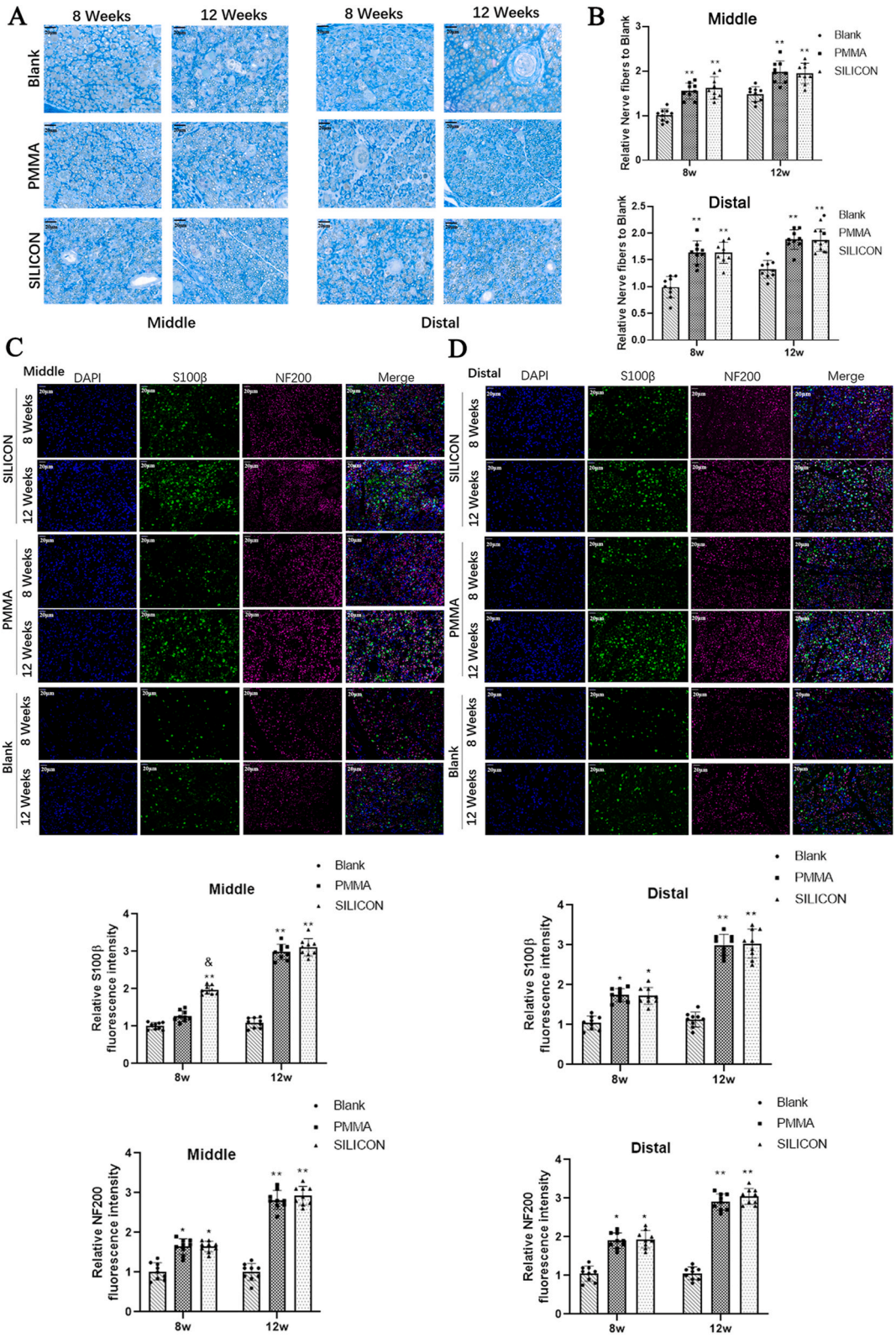

Fig. 5. Evaluation of nerve regeneration. (A, B) Toluidine staining was used to show the number of regenerated myelin axons. Scale bar = 100 μm. Immunofluorescence staining of S100β and NF-200 in the middle (C) and distal (D) anastomosis of the transplanted nerve 8 and 12 weeks post-surgery were performed to evaluate the axon growth. Scale bar = 50 μm. n = 3. $^{**}P < 0.01$ compared with blank.

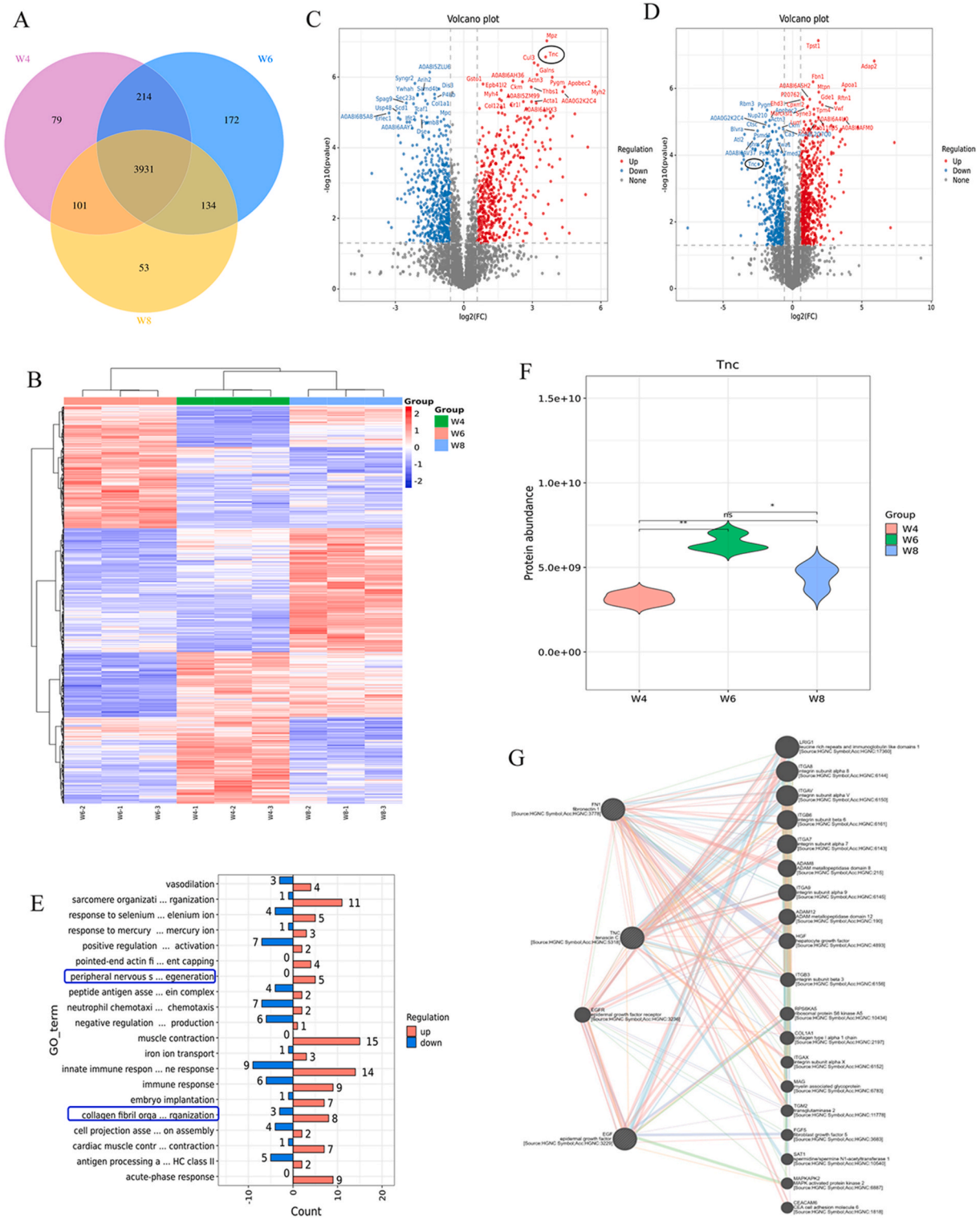

Fig. 6. Label-free whole proteomics assay of the biological membrane (4weeks, 6weeks and 8weeks) and bioinformatics analysis was performed. (A) The Venn diagram shows the overlap of proteins between different groups. (B) Protein expression level clustering heat map, 8-week (W8) biological membrane VS 6-week (W6) biological membrane VS 4-week (W4) biological membrane. (C) Differential proteins volcano map, 6-week (W6) biological membrane VS 4-week (W4) biological membrane. (D) Differential protein volcano map, 8-week (W8) biological membrane VS 6-week (W6) biological membrane. (E) Statistical map of the number of different proteins in biological processes. (F) Tnc expression in the biological membrane (W8 VS W6 VS W4). n = 3. ns, no significance; $*P < 0.05$, $**P < 0.01$. (G) Bioinformatics analysis of Tnc related proteins.

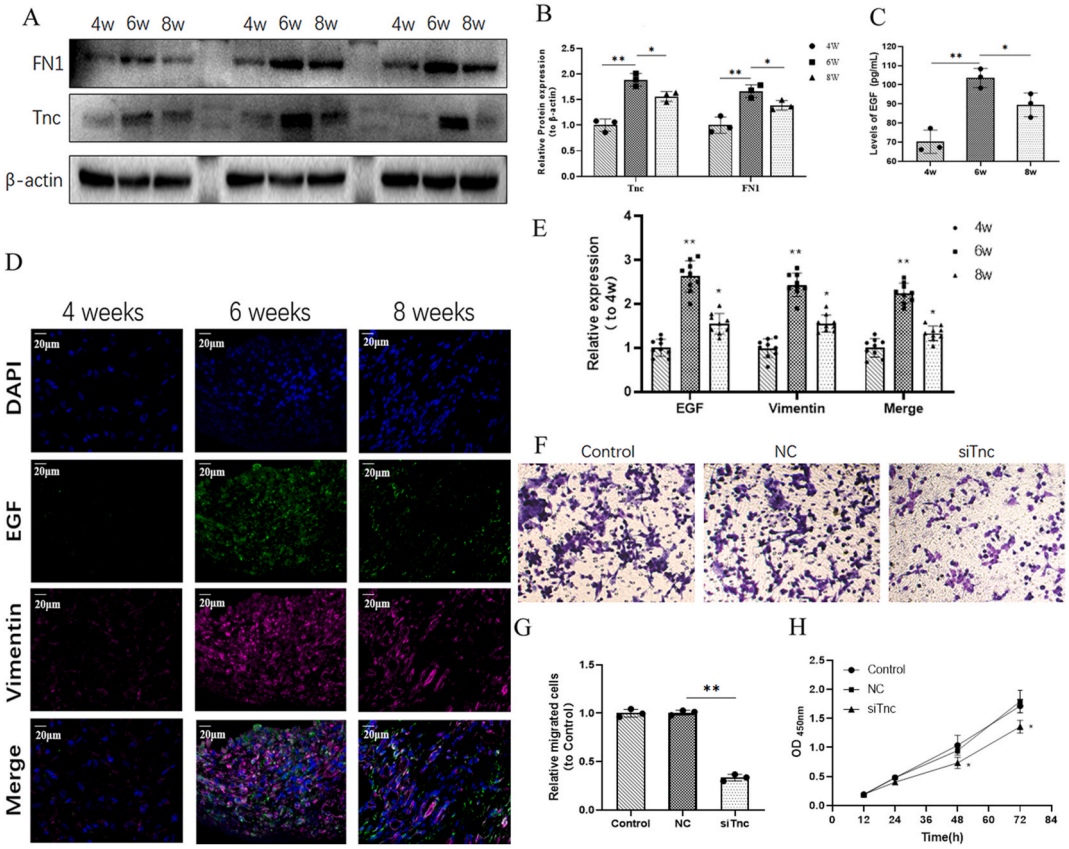

Fig. 7. EGF/Tnc/FN1 in the biological membrane and related experiments in vitro. (A) Western blot of Tnc/FN1 in the biological membrane in each group. (B) Western blot analysis of Tnc/FN1 in biological membrane. (C) EGF levels in the biological membrane in each group by ELISA. (D) Co-expression of EGF and Vimentin in the biological membrane from immunofluorescence. (E) Analysis of relative expression of EGF and Vimentin in the biological membrane. (F) Migration of Schwann cells of control, negatived control (NC) and Tnc siRNA (siTnc) co-cultured with EGF-treated fibroblasts assayed using transwell. (G) Quantification analysis of migrated cells in each group. (H) Cell proliferation of Schwann cells in each group were assayed using CCK8. OD450nm mediated cell viability. n = 3. $^{*}P < 0.05$, $^{**}P < 0.01$.

Based on the results of our experimental study, we can state the following. At 4, 6, and 8 weeks after operation, PMMA was placed near the nerve to form a biofilm which was rich in blood vessels and nerve growth related factors, and the content of neovascularization and factors was the highest at 6 weeks. This means that the optimal interval between surgeries is six weeks. Secondly, PMMA induced biofilm can significantly promote autogenous nerve transplantation to repair nerve defects, and the effect is not significantly different from that of silicon group. The biofilm is produced in vivo, non-immunogenic, has good biocompatibility, and its low cost is unmatched by other nerve conduits. Thirdly, the EGF/Tnc/FN1 may be one of the mechanisms by which biofilms promote nerve regeneration through increasing cell proliferation and migration of Schwann cells, further investigations were needed to validate the mechanisms of EGF/Tnc/FN1 in nerve regeneration. The present work lacked the critical tests as neurophysiological test and transmission electron microscopy (TEM) data to detect the thickness of myelin sheath, the diameter of myelinated axons and G ratio, which should be investigated in the further.

5. Conclusion

In conclusion, our study confirmed that PMMA-induced biofilms can better facilitate autologous nerve grafting to repair nerve defects and may be due to promotes Schwann cells migration and proliferation mediated by fibroblast-derived EGF/TNC/FN1. In addition, PMMA could induce the formation of biofilms with similar histological characteristics as silicone rods, and the histological and functional test results of the two biofilm-coated nerve grafts were similar. In special cases, such as severely contaminated limb open trauma, we consider using antibiotic-loaded PMMA to clear the infected lesion in the first stage and create a good biological microenvironment for the preparation of the nerve bed in the second stage. Secondly, in the treatment of perineural scar wounds, PMMA-induced biofilm can be used to repair nerve defects, and also create a good microenvironment for transplanted nerves to achieve better clinical transformation.

Funding

This study was provided by Wuxi Top Medical Expert Team of "Taihu Talent Program" (TTPJY2021).

Data availability statement

All data would be obtained from the corresponding author upon reasonable request.

Ethics approval

All the animal experiments were performed in accordance with the approval of the Animal Care and Use Committee of Wuxi 9th People's Hospital affiliated to Soochow University (KS2023059).

CRediT authorship contribution statement

Jun Wang: Writing – original draft, Methodology, Data curation. **YuXuan Hu:** Methodology, Formal analysis, Data curation. **Yuan Xue:** Methodology, Formal analysis, Data curation. **Kai Wang:** Methodology, Formal analysis, Data curation. **Dong Mao:** Formal analysis, Data curation. **Xiao-Yun Pan:** Formal analysis, Data curation. **YongJun Rui:** Project administration, Conceptualization.

Declaration of competing interest

The authors declare that they have no known competing financial interests or personal relationships that could have appeared to influence the work reported in this paper.

Appendix A. Supplementary data

Supplementary data to this article can be found online at https://doi.org/10.1016/j.heliyon.2024.e37231.

References

[1] N. Mokarram, et al., Immunoengineering nerve repair, Proc. Natl. Acad. Sci. U. S. A. 114 (2017) E5077–E5084.
[2] J. Sayanagi, et al., Combination of electrospun nanofiber sheet incorporating methylcobalamin and PGA-collagen tube for treatment of a sciatic nerve defect in a rat model, J Bone Joint Surg Am 102 (2020) 245–253.
[3] G.N. Panagopoulos, P.D. Megaloikonomos, A.F. Mavrogenis, The present and future for peripheral nerve regeneration, Orthopedics 40 (2017) e141–e156.
[4] T.M. Saffari, M. Bedar, C.A. Hundepool, A.T. Bishop, A.Y. Shin, The role of vascularization in nerve regeneration of nerve graft, Neural Regen Res 15 (2020) 1573–1579.
[5] V. Viateau, et al., Use of the induced membrane technique for bone tissue engineering purposes: animal studies, Orthop. Clin. N. Am. 41 (2010) 49–56.
[6] J.F. Soni, et al., Evaluation of silver nanoparticle-impregnated PMMA loaded with vancomycin or gentamicin against bacterial biofilm formation, Injury 54 (Suppl 6) (2023) 110649.
[7] A.C. Masquelet, F. Fitoussi, T. Begue, G.P. Muller, [Reconstruction of the long bones by the induced membrane and spongy autograft], Ann. Chir. Plast. Esthet. 45 (2000) 346–353.
[8] G. Lundborg, H.A. Hansson, Regeneration of peripheral nerve through a preformed tissue space. Preliminary observations on the reorganization of regenerating nerve fibres and perineurium, Brain Res. 178 (1979) 573–576.
[9] V. Penna, B. Munder, G.B. Stark, E.M. Lang, An in vivo engineered nerve conduit–fabrication and experimental study in rats, Microsurgery 31 (2011) 395–400.
[10] V. Penna, K. Wewetzer, B. Munder, G.B. Stark, E.M. Lang, The long-term functional recovery of repair of sciatic nerve transection with biogenic conduits, Microsurgery 32 (2012) 377–382.
[11] A.K. Yapici, Y. Bayram, H. Akgun, R. Gumus, F. Zor, The effect of in vivo created vascularized neurotube on peripheric nerve regeneration, Injury 48 (2017) 1486–1491.
[12] H. Takeuchi, et al., The efficacy of combining a vascularized biogenic conduit and a decellularized nerve graft in the treatment of peripheral nerve defects: an experimental study using the rat sciatic nerve defect model, Microsurgery 42 (2022) 254–264.
[13] C. Nau, et al., Alteration of Masquelet's induced membrane characteristics by different kinds of antibiotic enriched bone cement in a critical size defect model in the rat's femur, Injury 47 (2016) 325–334.
[14] T. Ozalp, A.C. Masquelet, [The role of creating a biological membrane in expediting nerve regeneration for peripheral nerve repairs], Acta Orthop. Traumatol. Turcica 42 (2008) 130–134.
[15] S.A. Zadegan, et al., Two-stage nerve graft in severe scar: a time-course study in a rat model, Arch Bone Jt Surg 3 (2015) 82–87.
[16] H. Liu, et al., Histological characteristics of induced membranes in subcutaneous, intramuscular sites and bone defect, Orthop Traumatol Surg Res 99 (2013) 959–964.
[17] E. de Mones, et al., Comparative study of membranes induced by PMMA or silicone in rats, and influence of external radiotherapy, Acta Biomater. 19 (2015) 119–127.
[18] T. Sagardoy, et al., Influence of external beam radiotherapy on the properties of polymethyl methacrylate-versus silicone-induced membranes in a bilateral segmental bone defect in rats, Tissue Eng. 24 (2018) 703–710.
[19] A.J. Lodge, et al., A novel bioresorbable film reduces postoperative adhesions after infant cardiac surgery, Ann. Thorac. Surg. 86 (2008) 614–621.
[20] D.W. Zochodne, The microenvironment of injured and regenerating peripheral nerves, Muscle Nerve Suppl 9 (2000) S33–S38.
[21] M. Salehirozveh, A.K. Kure Larsen, M. Stojmenovic, F. Thei, M. Dong, In-situ PLL-g-PEG functionalized nanopore for enhancing protein characterization, Chem. Asian J. 18 (2023) e202300515.
[22] Z. Jia, J. Choi, S. Lee, S.A. Soper, S. Park, Modifying surface charge density of thermoplastic nanofluidic biosensors by multivalent cations within the slip plane of the electric double layer, Colloids Surf. A Physicochem. Eng. Asp. 648 (2022).

[23] Z. Toth, et al., Masquelet technique: effects of spacer material and micro-topography on factor expression and bone regeneration, Ann. Biomed. Eng. 47 (2019) 174–189.
[24] C. Raza, H.A. Riaz, R. Anjum, N.U.A. Shakeel, Repair strategies for injured peripheral nerve: Review, Life Sci. 243 (2020) 117308.
[25] E. Liodakis, V.P. Giannoudis, S. Sehmisch, A. Jha, P.V. Giannoudis, Bone defect treatment: does the type and properties of the spacer affect the induction of Masquelet membrane? Evidence today, Eur. J. Trauma Emerg. Surg. 48 (2022) 4403–4424.
[26] Y. Kaizawa, et al., A nerve conduit containing a vascular bundle and implanted with bone marrow stromal cells and decellularized allogenic nerve matrix, Cell Transplant. 26 (2017) 215–228.
[27] T. Yamakawa, et al., Nerve regeneration promoted in a tube with vascularity containing bone marrow-derived cells, Cell Transplant. 16 (2007) 811–822.
[28] T. Yamamoto, et al., Trophic effects of dental pulp stem cells on Schwann cells in peripheral nerve regeneration, Cell Transplant. 25 (2016) 183–193.
[29] T. Gordon, The role of neurotrophic factors in nerve regeneration, Neurosurg. Focus 26 (2009) E3.
[30] A.C. Lee, et al., Controlled release of nerve growth factor enhances sciatic nerve regeneration, Exp. Neurol. 184 (2003) 295–303.
[31] D.A. Tiangco, K.C. Papakonstantinou, K.A. Mullinax, J.K. Terzis, IGF-I and end-to-side nerve repair: a dose-response study, J. Reconstr. Microsurg. 17 (2001) 247–256.
[32] H. Yu, et al., Improvement of peripheral nerve regeneration in acellular nerve grafts with local release of nerve growth factor, Microsurgery 29 (2009) 330–336.
[33] V.J. Vieira, et al., Vascular endothelial growth factor overexpression positively modulates the characteristics of periprosthetic tissue of polyurethane-coated silicone breast implant in rats, Plast. Reconstr. Surg. 126 (2010) 1899–1910.
[34] B. Wang, et al., The HIF-1α/EGF/EGFR signaling pathway facilitates the proliferation of Yak alveolar type II epithelial cells in hypoxic conditions, Int. J. Mol. Sci. 25 (2024).
[35] X. Lan, et al., Fibronectin mediates activin A-promoted human trophoblast migration and acquisition of endothelial-like phenotype, Cell Commun. Signal. : CCS 22 (2024) 61.
[36] M. Kitada, T. Murakami, S. Wakao, G. Li, M. Dezawa, Direct conversion of adult human skin fibroblasts into functional Schwann cells that achieve robust recovery of the severed peripheral nerve in rats, Glia 67 (2019) 950–966.
[37] Z. Zhang, et al., Fibroblast-derived tenascin-C promotes Schwann cell migration through β1-integrin dependent pathway during peripheral nerve regeneration, Glia 64 (2016) 374–385.
[38] L. Liu, G.P. Shi, CD31: beyond a marker for endothelial cells, Cardiovasc. Res. 94 (2012) 3–5.
[39] R.M. Menorca, T.S. Fussell, J.C. Elfar, Nerve physiology: mechanisms of injury and recovery, Hand Clin. 29 (2013) 317–330.
[40] M.K.B. Abdulaziz, et al., Two-stage reconstruction of hand extensor tendons using silicon rods, Plast Reconstr Surg Glob Open 9 (2021) e3858.
[41] D. Pan, S.E. Mackinnon, M.D. Wood, Advances in the repair of segmental nerve injuries and trends in reconstruction, Muscle Nerve 61 (2020) 726–739.
[42] M. Siemionow, et al., Peripheral nerve defect repair with epineural tubes supported with bone marrow stromal cells: a preliminary report, Ann. Plast. Surg. 67 (2011) 73–84.
[43] F. Bianchi, et al., Rapid and efficient differentiation of functional motor neurons from human iPSC for neural injury modelling, Stem Cell Res. 32 (2018) 126–134.
[44] C.K. Franz, U. Rutishauser, V.F. Rafuse, Intrinsic neuronal properties control selective targeting of regenerating motoneurons, Brain 131 (2008) 1492–1505.
[45] K. Wang, et al., Enhanced vascularization in hybrid PCL/gelatin fibrous scaffolds with sustained release of VEGF, BioMed Res. Int. 2015 (2015) 865076.
[46] A. Di Maio, et al., In vivo imaging of dorsal root regeneration: rapid immobilization and presynaptic differentiation at the CNS/PNS border, J. Neurosci. 31 (2011) 4569–4582.
[47] Y. Qian, et al., 3D melatonin nerve scaffold reduces oxidative stress and inflammation and increases autophagy in peripheral nerve regeneration, J. Pineal Res. 65 (2018) e12516.
[48] J. Choi, et al., Better nerve regeneration with distally based fascicular turnover flap than with conventional autologous nerve graft in a rat sciatic nerve defect model, J. Plast. Reconstr. Aesthetic Surg. 73 (2020) 214–221.